Comparison of the ^{12}C$(e,e'p)$ cross section at low momentum transfer with a relativistic calculation

T. Tamae,* Y. Sato, T. Yokokawa,† Y. Asano, M. Kawabata, O. Konno,‡ I. Nakagawa,§
I. Nishikawa, K. Hirota,‖ and H. Yamazaki
Laboratory of Nuclear Science, Graduate School of Science, Tohoku University, Mikamine, Taihaku-ku, Sendai 982-0826, Japan

R. Kimura, H. Miyase, and H. Tsubota
Department of Physics, Graduate School of Science, Tohoku University, Aramaki, Aoba, Sendai 980-8578, Japan

C. Giusti and A. Meucci
Dipartimento di Fisica Nucleare e Teorica, Università di Pavia and Istituto Nazionale di Fisica Nucleare, Sezione di Pavia, I-27100 Pavia, Italy

(Received 17 September 2009; published 1 December 2009)

The $(e,e'p_0)$ cross section of ^{12}C has been measured at an energy transfer of 60 MeV and a momentum transfer of 104.4 MeV/c using a 197.5 MeV continuous electron beam. The cross section at missing momenta between 181.5 and 304.8 MeV/c obtained from the experiment is compared with theoretical calculations based on the relativistic distorted-wave impulse approximation with and without meson-exchange currents (MEC). The contribution of MEC due to the seagull current is large in the high-missing-momentum region, in particular for the longitudinal component. The cross sections calculated using three different current-conserving operators (cc1, cc2, and cc3) are similar, in contrast to the (γ,p) reaction, where the operators give very different results. The shape of the measured cross section is well described by the calculations, whereas its magnitude is slightly smaller than that described by the calculations.

DOI: 10.1103/PhysRevC.80.064601 PACS number(s): 24.10.Jv, 24.50.+g, 25.30.Rw, 27.20.+n

I. INTRODUCTION

Electromagnetic one-nucleon emission reactions have provided a wealth of information concerning various aspects of the reaction mechanism. The $(e,e'p)$ reaction in the quasielastic region is well described within the framework of the direct knockout (DKO) model. This model is based on the assumption that a virtual photon couples to a single proton in the target nucleus. A theoretical approach based on the nonrelativistic distorted-wave impulse approximation (DWIA) can provide an excellent description of the shape of the experimental recoil-momentum distributions for states corresponding to specific peaks in the excitation-energy spectrum of the residual nucleus, in a wide range of nuclei and in different kinematics, at four-momentum transfer below 500 MeV/c [1–3]. The spectroscopic factor is determined by scaling the theoretical prediction to the experimental data. In such analyses, a 30%–40% quenching of the spectroscopic factors compared with mean-field values has been observed.

Recently, the $(e,e'p)$ reaction has been studied extensively in a fully relativistic DWIA (RDWIA) framework [4–11]. In addition, RDWIA calculations can provide a good description of the experimental results at medium momentum transfer. The spectroscopic factors extracted from the RDWIA approach are 10%–20% larger than those from the nonrelativistic DWIA analysis. Moreover, the relativistic approach is recognized as being necessary for the analysis of data at high momentum transfer [4–13].

The reaction mechanism of the (γ,p) reaction above the giant resonance region has been the subject of longstanding discussion. In the nonrelativistic approach [14–21], only a fraction of the measured (γ,p) cross section is given by the DKO process, and a meaningful contribution is produced by meson-exchange currents (MEC), which, in contrast, do not seriously affect the quasielastic $(e,e'p)$ cross sections [21–24]. The effects of MEC and Δ excitations in $(e,e'p)$ reactions have recently been studied within a semirelativistic model in Ref. [25], where a moderate dependence on MEC was predicted only at a high missing momentum.

Substantially different results are obtained from the relativistic approaches for the (γ,p) reaction [6,26–29]. RDWIA calculations are close to the measured cross sections in light nuclei at photon energies below 100 MeV. This means that the contribution of MEC may not be large in the relativistic framework. Actually, it has been shown [21,29] that the contribution of the two-body current corresponding to the seagull term affects the (γ,p) cross section less than in the nonrelativistic calculations, although the MEC contribution becomes more important with increasing photon energy and missing momentum [29].

*tamae@lns.tohoku.ac.jp
†Present address: Iwanami Shoten Publishers, 2-5-5, Hitotsubashi, Chiyoda-ku, Tokyo 101-8002, Japan.
‡Present address: Department of Electrical Engineering, Ichinoseki National College of Technology, Hagiso, Ichinoseki 021-8511, Japan.
§Present address: RIKEN Nishina Center, Wako, Saitama 351-0198, Japan.
‖Present address: RIKEN Radiation Lab., Wako, Saitama 351-0198, Japan.

The choice of the electromagnetic operator for the one-body current has also been a longstanding problem [8,12,28–31]. No unambiguous approach is available at present to deal with off-shell nucleons. Current-conserving operators (cc1, cc2, and cc3) [30], which are usually used in relativistic calculations, are equivalent to each other for on-shell particles owing to the Gordon identity, but give different results when applied to off-shell nucleons. Although the differences are small in the kinematics for the quasielastic $(e,e'p)$ reaction, large differences are found for the (γ,p) reaction [28].

When discussing the role of components such as the current operator and MEC in $(e,e'p)$ and (γ,p) reactions, we must consider that these experiments are usually carried out under different kinematical conditions. In the (γ,p) reaction, the energy transfer ω and three-momentum transfer $\boldsymbol{q}$ are constrained by the condition $\omega = |\boldsymbol{q}| = E_\gamma$, and the mismatch between the momentum transfer and the momentum of the outgoing nucleon $\boldsymbol{p}'$ is quite large. Thus, only high values of the missing momentum $p_m = |\boldsymbol{p}_m| = |\boldsymbol{q} - \boldsymbol{p}'|$, which is the recoil momentum of the residual nucleus, can be explored by measuring the cross section for different values of the scattering angle of the outgoing proton. In the $(e,e'p)$ reaction, ω and $\boldsymbol{q}$ can be varied independently, and all possible values of the missing momentum can be explored using suitable kinematics. The $(e,e'p)$ data of Refs. [32,33] were obtained in parallel kinematics, where the momentum of the outgoing proton (and thus also its kinetic energy) is fixed and is taken parallel or antiparallel to the momentum transfer. Different values of the missing momentum are obtained by varying the electron scattering angle and, therefore, the momentum transfer. The energies and momentum transfers for those $(e,e'p)$ data are higher than for the (γ,p) data of Refs. [15–19,34–36]. Also, the energy of the outgoing proton is higher. Thus, the cross sections might show a different sensitivity to final-state interactions, which are usually treated in the DWIA and RDWIA approaches by means of phenomenological energy-dependent optical potentials.

A new $(e,e'p)$ experiment at low momentum transfer kinematically designed to be similar to the (γ,p) reaction will bridge the photon point and high-momentum-transfer experiments. It will provide us with information regarding the momentum transfer dependence of relativistic effects, MEC, and the choice of the current operator, by filling the gap between experiments at high momentum transfer and ones at the photon point. The similarity of the kinematics to the (γ,p) reaction is very important in this approach for removing ambiguities caused by, to some extent, final-state interactions. As the present $(e,e'p)$ reaction is dominated by the longitudinal component, in contrast to the (γ,p) reaction, which is purely transverse, it will be useful to disentangle the contribution of MEC. In the present $^{12}\mathrm{C}(e,e'p)$ experiment, we chose an energy transfer of $\omega = 60$ MeV, that is, the same energy as for the $^{12}\mathrm{C}(\gamma,p)$ data of Refs. [15–17,35,36]. Thus, the energy of the outgoing proton is also the same and, as a consequence, the final-state interactions are expected to be similar to the (γ,p) reaction. The momentum transfer of the present experiment is 104.4 ± 1.3 MeV/c. The azimuthal angle between the electron scattering plane and the reaction plane is taken to be $\phi_p = 90^\circ$, to eliminate the longitudinal-transverse (LT) interference term in the cross section. Although the LT term includes interesting physics, it complicates the discussion when we compare the present result with the (γ,p) reaction. The transverse-transverse term R_{TT} is smaller than R_L and R_T, as shown in Sec. IV.

The experimental procedure is presented in Sec. II. In Sec. III, the experimental data are shown and compared with relativistic calculations with and without MEC. A summary and conclusions are given in Sec. IV.

II. EXPERIMENT

The experiment was performed using a continuous electron beam from a stretcher-booster ring (STB) [37] at Tohoku University. The beam is extracted from the ring using monochromatic extraction [37,38]. In this method, the energy spread of the injected beam is chosen to be equal to the energy loss that occurs between two successive injections, and electrons are extracted at the lowest energy after losing energy from synchrotron radiation. In the present experiment, a beam of 198.0 ± 0.5 MeV was injected into the ring after being momentum-analyzed in a nondispersive achromatic magnetic analyzing system consisting of a quadrupole magnet between two bending magnets, whose magnetic field was monitored using a nuclear magnetic resonance (NMR) method. The energy of the electron beam supplied to the experiment was tuned at 197.5 MeV, and scattered electrons of 137.5 ± 4 MeV were measured at 30°. The corresponding energy and momentum transfer are $\omega = 60 \pm 4$ MeV and $|\boldsymbol{q}| = 104.4 \pm 1.3$ MeV/c, respectively. The beam intensity was in the range of 500–700 nA, which was monitored using a secondary-electron monitor (SEM) downstream of the target. The experimental setup is similar to the one described in previous papers [39,40]. Electrons scattered with a 9.2 mg/cm^2 thick natural carbon foil were momentum-analyzed using a double-focusing magnetic spectrometer having a solid angle of 2.9 msr and detected by means of a vertical drift chamber (VDC) in the focal plane and two layers of plastic scintillators. The magnetic field of the spectrometer was monitored using NMR.

Ejected protons were measured using counter telescopes composed of four surface-barrier-type silicon solid-state detectors (one 50-μm- and three 1-mm-thick detectors) at eight angles ϑ_p with respect to the momentum transfer direction out of the plane, $\phi_p = 90^\circ$, in order to explore different values of the missing momentum. Charged particles reaching at least the second layer of the telescope were used for analysis. Particle identification and absolute energy calibration for each detector were achieved using the $\Delta E - E$ technique [40]. The energy of charged particles was reduced from energies dissipated in the detectors, using the Bethe-Bloch formula. The values of sensitive depth in quality assurance data were used in the calculation. In the present experiment, energies of measured protons were in the range of 40–48 MeV, which are too high to be stopped by three layers of detectors. In such a case, a good energy resolution cannot be achieved because only a fraction of the energy is dissipated in the detectors.

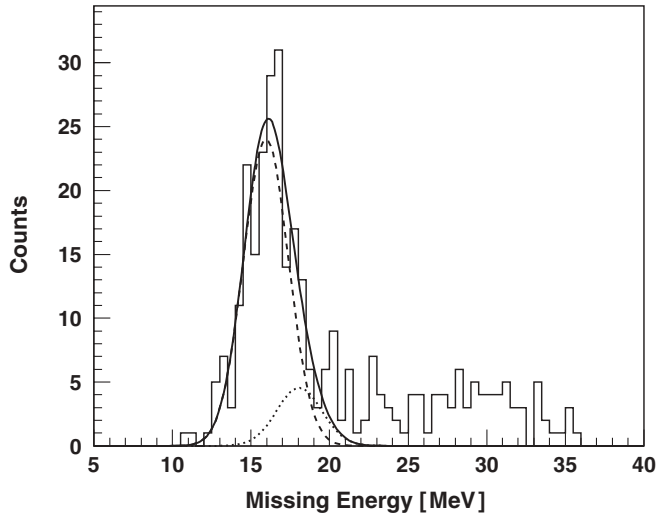

FIG. 1. An example of the missing energy spectrum, which was measured at the momentum transfer direction. Events between 13 and 19 MeV were separated into $(e,e'p_0)$ and $(e,e'p_1)$ components by fitting the data with two Gaussians using a maximum-likelihood method. The dashed and dotted curves represent the $(e,e'p_0)$ and $(e,e'p_1)$ components, respectively, and the solid curve gives their sum.

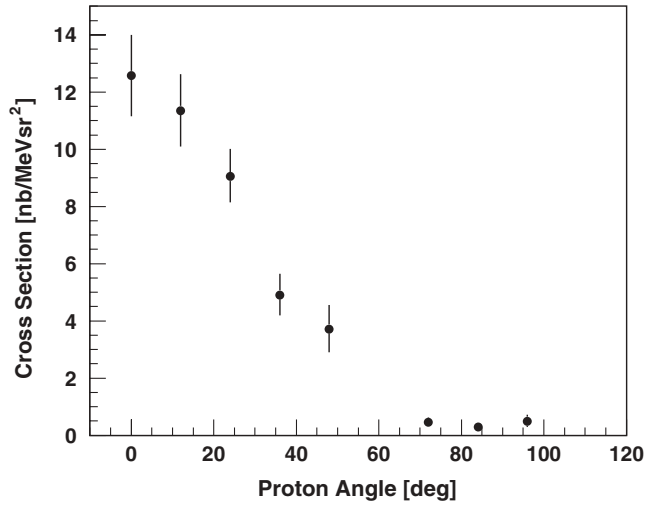

FIG. 2. Cross section of the ^{12}C(e,$e'p_0$) reaction as a function of the angle ϑ_p between the outgoing proton and the momentum transfer.

A 3-mm-thick aluminum disk was installed in front of each telescope to improve the energy resolution by degrading the proton energy. The thickness was optimized so that the highest resolution was obtained for measurement of the proton energy. A Monte Carlo calculation showed that the fraction of protons lost due to multiple scattering is negligible and the energy broadening is ultimately 300 keV. The energy dissipated in the degrader was calculated using the Bethe-Bloch formula and summed to achieve initial proton energies. The solid angle of each telescope was defined using an iron collimator to be 4.93 msr.

Because of problems in obtaining data concerning the VDC, we used information describing the time difference of signals at both ends of the backup scintillation counters to fix the momentum of scattered electrons. The resulting energy resolution in missing energy spectra, approximately 3 MeV at full width half maximum (FWHM), is not sufficient to completely separate events for the transition to the ground state, $(e, e' p_0)$, of the residual state and those to the first excited state, $(e, e' p_1)$, as shown in Fig. 1. Events between $E_m = 13$ and 19 MeV of each spectrum were separated into the two states using a maximum-likelihood method, where the amplitudes of two Gaussians and their width were treated as parameters. The uncertainties of the fitting were also calculated using the same method.

A combination of the solid angle of the spectrometer, the target thickness, and efficiencies of the SEM and electron detectors was deduced from the normalization of elastic scattering data to existing ones. The elastic scattering cross section measured at 65° using an electron beam of 197.5 MeV was used for the normalization, after radiative corrections corresponding to the Schwinger, bremsstrahlung, and collision corrections were applied to the data in the same way as in Refs. [41,42]. The form factor at $|\boldsymbol{q}| = 211.1\,\mathrm{MeV}/c$ was calculated from a three-parameter Gaussian charge distribution [43], which gives a very close fit to the form factor below $300\,\mathrm{MeV}/c$ deduced from the cross sections in Refs. [44,45]. The cross section was also calculated using the phase-shift analysis code DREPHA 11 [46] employing the parameter sets described in Refs. [44,45]. The values obtained from fitting and phase-shift calculations agree within 3%, and the value obtained by the fitting, 3.50 μb/sr, is used for normalization. The radiative correction to the $(e, e' p_0)$ reaction was carried out using a Monte Carlo simulation program AEEXB [47]. The resultant $(e, e' p_0)$ cross section as a function of the angle ϑ_p (between the outgoing proton and the momentum transfer) is shown in Fig. 2 and listed in Table I. The errors were obtained by combining in quadrature the statistical error, the fitting error of the missing-energy spectrum, and the error of the normalization of the elastic scattering cross section. The angular distribution shows a strong forward peak, and the cross sections at backward angles ($\vartheta_p > 70°$) are much smaller.

TABLE I. Double differential cross section and reduced cross section of the $(e, e' p_0)$ reaction.

(θ_p, ϕ_p)	p_m (MeV/c)	Differential cross section (nb/MeV/sr^2)	Reduced cross section $\rho(p_m)$ (MeV/c)$^{-3}$
(0°,–)	181.5	$12.58\,^{+1.42}_{-1.41}$	$(3.78\,^{+0.43}_{-0.42}) \times 10^{-9}$
(12°, 90°)	184.8	$11.36\,^{+1.27}_{-1.26}$	$(3.41\,^{+0.38}_{-0.38}) \times 10^{-9}$
(24°, 90°)	194.4	$9.05\,^{+0.90}_{-0.96}$	$(2.69\,^{+0.27}_{-0.29}) \times 10^{-9}$
(36°, 90°)	208.8	$4.91\,^{+0.72}_{-0.74}$	$(1.44\,^{+0.21}_{-0.22}) \times 10^{-9}$
(48°, 90°)	226.6	$3.72\,^{+0.81}_{-0.83}$	$(1.08\,^{+0.24}_{-0.24}) \times 10^{-9}$
(72°, 90°)	266.4	$0.45\,^{+0.16}_{-0.18}$	$(1.28\,^{+0.46}_{-0.51}) \times 10^{-10}$
(84°, 90°)	286.1	$0.30\,^{+0.14}_{-0.16}$	$(0.86\,^{+0.40}_{-0.46}) \times 10^{-10}$
(96°, 90°)	304.8	$0.49\,^{+0.20}_{-0.24}$	$(1.41\,^{+0.58}_{-0.69}) \times 10^{-10}$

III. DISCUSSION

The unpolarized $(e,e'p)$ cross section in the first Born approximation can be expressed in terms of four response functions $R_{\lambda\lambda'}$ as [3,7]

$$\sigma_{e,e'p} \equiv \frac{d^3\sigma}{d\omega d\Omega_e d\Omega_p} = \frac{K}{(2\pi)^3}\sigma_M[v_L R_L + v_T R_T + v_{LT} R_{LT}\cos(\phi_p) + v_{TT} R_{TT}\cos(2\phi_p)], \quad (1)$$

where σ_M is the Mott cross section, $K = |\boldsymbol{p}'|E'_p$ is a kinematical factor, and ϕ_p is the azimuthal angle between the electron scattering plane and the $(\boldsymbol{q}, \boldsymbol{p}')$ plane. The coefficients $v_{\lambda\lambda'}$ are obtained from the lepton tensor components and depend only upon the electron kinematics [3]. The response functions $R_{\lambda\lambda'}$ represent the response of the nucleus to the longitudinal (L) and transverse (T) components of the electromagnetic interaction. They are obtained from suitable combinations of the components of the hadron tensor [3] and are given by bilinear combinations of the transition matrix elements of the nuclear charge-current operator between initial and final nuclear states.

In the plane-wave impulse approximation (PWIA), the $(e,e'p)$ cross section can be factorized in the form [30]

$$\sigma_{e,e'p} = K\sigma_{e,p}S(E_m, p_m), \quad (2)$$

where $\sigma_{e,p}$ is the off-shell electron-proton scattering cross section, and $S(E_m, p_m)$ is the diagonal spectral function [3], which gives the joint probability of removing a nucleon with initial momentum p_m and separation energy E_m from the target nucleus. At each value of E_m, the momentum dependence of the spectral functions corresponds to the momentum distribution of the quasihole state produced in the target at that energy. Data for the $(e,e'p)$ reaction are usually presented in terms of the reduced cross section for specific values of E_m, as defined by

$$\rho_{e,e'p}(E_m, p_m) = \frac{\sigma_{e,e'p}}{K\sigma_{e,p}}, \quad (3)$$

which gives the momentum distribution of the proton in the nucleus in the PWIA. Although the factorization of Eq. (2) is valid only for the nonrelativistic PWIA [31], the definition of Eq. (3) is useful to compare experimental results measured in different kinematics. The experimental reduced cross section, in fact, also contains the effects of final-state interactions, which are included in the DWIA by means of phenomenological optical potentials, as well as other possible contributions beyond the DWIA.

The $(e,e'p_0)$ differential cross section measured in the present experiment is listed in Table I, together with the reduced cross section obtained from Eq. (3), using the cc2 prescription [30] for $\sigma_{e,p}$. In the present kinematics, the results using cc1 and cc2 prescriptions given in Ref. [30] differ by no more than 2%. In Fig. 3, our reduced cross section (closed circles) is compared with the results of the $(e,e'p_0)$ experiment at NIKHEF-K [32] (open triangles) measured in parallel kinematics at higher momentum transfers, ranging from 155 to 519 MeV/c, and with those of the (γ,p) experiments [16] (open circles). The present data cover a missing-momentum range higher than the region covered in Ref. [32] and the whole range of the (γ,p) experiment. The reduced cross section obtained from the present experiment is approximately one-half of the $(e,e'p)$ data at higher momentum transfers. It is also smaller than the (γ,p) data.

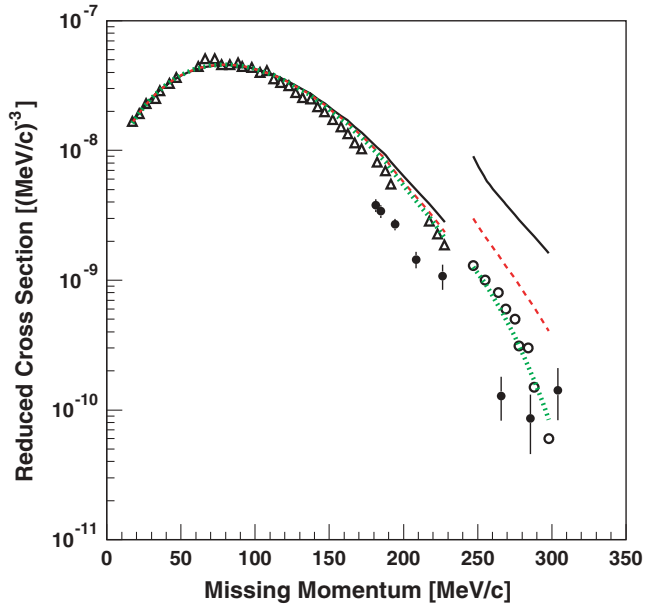

FIG. 3. (Color online) Reduced cross section of ^{12}C$(e,e'p_0)$ and (γ, p_0) reactions as a function of the missing momentum. Closed circles show the results of the present $(e,e'p_0)$ experiment at $|\boldsymbol{q}| =$ 104.4 MeV/c. Open triangles and open circles represent the results of the ^{12}C$(e,e'p_0)$ [32] at higher momentum transfers, ranging from 155 to 519 MeV/c, and (γ,p_0) [16] reactions, respectively. Curves show the RDWIA calculations corresponding to them. Solid (black), dashed (red), and dotted (green) curves are calculations for cc1, cc2, and cc3 current operators, respectively.

The present data are compared with the RDWIA calculations. The theoretical approach is the same as that described in Refs. [7,28,29]. The relativistic bound-state wave functions have been obtained using NL2 parameters [48]. The scattering state is calculated by means of the energy-dependent and A-dependent EDAD1 complex phenomenological optical potential reported in Ref. [49], which is fitted to proton elastic scattering data from several nuclei in the energy range of 20–1040 MeV. For the one-body current operator, since there is no unambiguous prescription for involving off-shell nucleons, the results given by the three current-conserving prescriptions (cc1, cc2, and cc3) [30] are compared. The spectroscopic factors are obtained by fitting the calculations with the ^{12}C$(e, e' p_0)$ data at higher momentum transfer measured at NIKHEF-K [32]; they are $S_{\rm cc1} = 1.90$, $S_{\rm cc2} = 2.02$, and $S_{\rm cc3} = 2.09$ for the three current-conserving prescriptions (cc1, cc2, cc3), respectively. Although the data can be well fitted by the calculations at $p_m \leqslant 120$ MeV/c, they overestimate the experimental values in the higher missing-momentum region, as shown in Fig. 3; the enhancement is 31%, 22%, and 16% around 180 MeV/c for cc1, cc2, and cc3, respectively. The use of NL-SH parameters for calculation of the bound-state wave function, which were used in Ref. [28], gives more enhancement there. The reduced cross sections of the (γ,p)

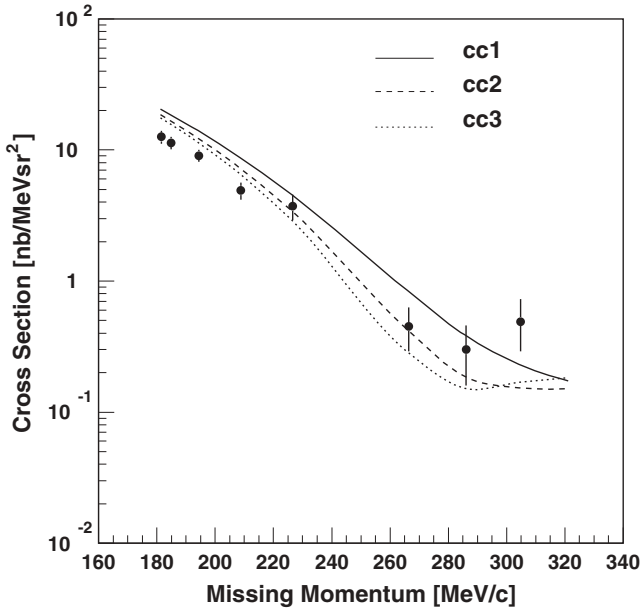

FIG. 4. The ^{12}C(e,$e'p_0$) cross section of the present experiment as a function of the missing momentum. Solid, dashed, and dotted lines are the RDWIA results using the cc1, cc2, and cc3 one-body current operators, respectively. The corresponding spectroscopic factors have been applied to the calculations.

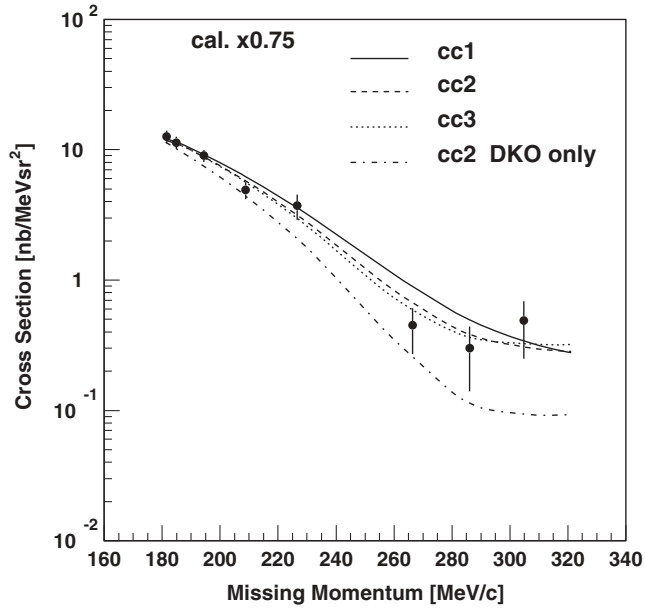

FIG. 5. The ^{12}C(e,$e'p_0$) cross section of the present experiment as a function of the missing momentum, in comparison with the relativistic calculations involving the one-body + seagull current. Solid, dashed, and dotted lines are obtained using the cc1, cc2, and cc3 one-body current operators, respectively. The dot-dashed line is calculated using the one-body cc2 current without the seagull term. Corrections described in the text have been applied to all the theoretical calculations. A further factor of 0.75 is applied to normalize them to the present experimental value at the lowest missing momentum.

reaction calculated in the RDWIA calculation using the same potential parameters and the same spectroscopic factors are also shown in Fig. 3. Large and even huge current ambiguities are found for cc1, cc2, and cc3 operators; the cc3 current gives a satisfactory agreement, whereas the cc2 current overestimates the data by a factor of 2, and the cc1 current gives a result of almost an order of magnitude larger than the data. It should be noted that the results are slightly different from those in Ref. [28] owing to the use of a different parametrization for the bound-state wave function.

Figure 4 shows a comparison of the present data with the RDWIA calculations, where the previously obtained spectroscopic factors have been applied to the calculations. The measured cross section decreases with increasing missing momentum, but the decrease is slower than in the theoretical results. The differences in the calculations involving the three different current operators are sizable and increase with the missing momentum, although they are much smaller than those in the (γ, p) reaction. The cross section obtained using the cc1 current is enhanced with respect to that using cc2, whereas the results obtained using cc2 and cc3 are closer to each other. Although it is difficult to discuss the choice of the current operator at $p_m \geqslant 250\,\mathrm{MeV}/c$ due to large errors of the data, all the calculations overestimate the data by a factor of about 1.5 at the lowest value of the missing momentum.

Figure 5 shows a comparison of our data with the relativistic calculations where the two-body seagull current is also included [29,50]. The cross sections calculated using the cc1, cc2, and cc3 prescriptions for the one-body current operator are displayed. The result obtained using only the one-body cc2 current is also shown in the figure for comparison. All the theoretical results have been multiplied by the corresponding spectroscopic factors. As shown in Fig. 3, the RDWIA calculations overestimate NIKHEF data around 180 MeV/c; to remove the overestimation, theoretical values have been decreased by 31%, 22%, and 16% for cc1, cc2, and cc3 prescriptions, respectively. After these corrections, resultant theoretical values overestimate the present experimental one at 180 MeV/c by about 30%; in Fig. 5, the theoretical values are multiplied by a further factor of 0.75 to normalize the calculated cross sections to the present data at the lowest values of the missing momentum. When the seagull term is added in the nuclear current and the overestimation of the calculations at 180 MeV/c is corrected, the differences among the three calculations are reduced. The seagull contribution enhances the cross section, and this enhancement is larger at higher values of the missing momentum. Thus, the shapes of all three calculations turn out to be in closer agreement with the data, although their absolute values slightly overestimate the data over the whole momentum range explored in the present experiment.

The contribution of the seagull current in the relativistic calculation is important in the present situation of low momentum transfer for the (e, $e'p_0$) reaction and is larger than that at higher momentum transfer in both the nonrelativistic [21] and relativistic [29] approaches. It is also larger than that for the ^{12}C(γ, p) reaction at $E_\gamma = 60\,\mathrm{MeV}$ in the same relativistic approach [29]. We must consider, however, that, owing to current conservation, only the transverse components

of the two-body current are included in the nonrelativistic approach [21]. Their effect on the transverse components of the nuclear response in the nonrelativistic approach is in general larger than that in the relativistic approach. Thus, for the (γ, p) reaction, where only the transverse current contributes, MEC effects are found to be smaller in the relativistic calculations than in the nonrelativistic calculations [29]. In the relativistic framework, the two-body current is included both in the longitudinal and transverse components, and it affects all the response functions. The effect of the seagull current on the separated response functions for the present $^{12}C(e, e' p_0)$ reaction is shown in Fig. 6 for the cc2 one-body current operator. Similar results are obtained with cc1 and cc3. The seagull term produces a strong enhancement of the longitudinal response at large missing momenta, which is mainly responsible for the change of shape given by MEC in the calculated cross sections shown in Fig. 4. This effect occurs only in the relativistic calculation and can thus be considered as a relativistic effect.

Only the contribution of MEC due to the seagull diagrams was included in the present relativistic calculations. Although these terms should represent the main contribution of MEC in the considered kinematics, other diagrams involving one-pion exchange should also be included in the model. In the nonrelativistic calculations, the pion-in-flight terms reduce the effect of the seagull current, while the Δ-isobar current is not important in the present kinematics. Although similar effects can also be expected in the relativistic approach, only an explicit calculation would give a clear and quantitative answer concerning the role of two-body currents.

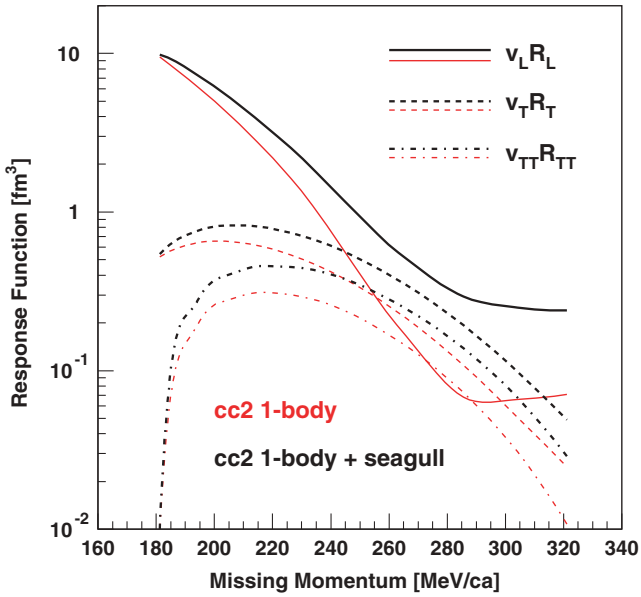

FIG. 6. (Color online) Separated response functions calculated in RDWIA for the cc2 current operator. Thick (black) lines represent the results obtained including the seagull contribution, and thin (red) lines show those without it. Solid, dashed, and dash-dotted lines show the longitudinal, transverse, and transverse-transverse components of the response function, respectively. The spectroscopic factor is not applied in the calculation.

IV. SUMMARY AND CONCLUSION

The cross section of the $^{12}C(e,e'p_0)$ reaction has been measured at low energy and low momentum transfer, $\omega = 60$ MeV and $|\boldsymbol{q}| = 104.4$ MeV/c, respectively, in the missing-momentum range between 181.5 and 304.8 MeV/c. The reduced cross section is one-half that of the $^{12}C(e,e'p)$ reaction at higher momentum transfers [32] and one-half that of the $^{12}C(\gamma, p)$ reaction at $E_\gamma = 60$ MeV [16].

The experimental cross section has been compared with RDWIA calculations with and without MEC, where the spectroscopic factors have been obtained from the $(e, e' p_0)$ cross section measured at higher momentum transfers. The theoretical results without MEC overestimate the cross section of the present experiment by a factor of about 1.5 at around $p_m = 180$ MeV/c, and those including MEC do the same throughout the missing-momentum region covered by this experiment. As shown in Fig. 3, the RDWIA calculations overestimate the NIKHEF data by 15%–30% in the region of $p_m = 180$–220 MeV/c. This suggests that some part of the discrepancy in the present experiment may be attributed to the overestimation of the momentum distribution calculated with the RDWIA using the NL2 parameters. The correction for this discrepancy also improves the agreement between the present experiment and the RDWIA calculations. After inclusion of MEC and the aforementioned correction, the shape of the $^{12}C(e, e' p_0)$ cross section measured at $\omega = 60$ MeV and $|\boldsymbol{q}| = 104.4$ MeV/c is well described with the RDWIA calculations, although there remains a small difference in the absolute values.

Only the MEC contribution due to the seagull current is included in the calculations. Its effect is large at high missing momenta, where it produces an enhancement that improves the agreement in terms of the shape of the cross section. This effect is due to the combined increase of both the longitudinal and transverse components of the nuclear response. In particular, the longitudinal response is increased up to approximately one order of magnitude by the seagull current at the highest considered values of the missing momentum. Although the seagull term should give the main contribution of MEC in the kinematics of the present experiment, the inclusion of other terms, in particular of the pion-in-flight current, would allow a more reliable quantitative comparison with data.

In the case of the $^{12}C(\gamma, p)$ reaction, the RDWIA calculations using the three different current operators (cc1, cc2, and cc3) produce huge differences, as shown in Fig. 3. The result using the cc3 operator was close to the experimental data, whereas a large or huge overestimation was obtained using the cc2 and cc1 currents [28]. The discrepancy between the present $(e, e' p_0)$ reaction is much smaller than that for the (γ, p) reaction. In contrast to the $(e, e' p_0)$ and (γ, p) reactions, the RDWIA calculation underestimates the $^{12}C(\gamma, n)$ cross section at 60 MeV by one order of magnitude, even after the MEC effect (seagull term) is added to the DKO process [29]. These results suggest that more complicated effects such as a rescattering process and/or correlations are needed to describe the data in this energy region. It was shown recently [51] that reduced cross sections for the transverse

part of the $^{12}C(e,e'p)$ reaction, which were obtained from a Rosenbluth separation at higher energies, and the (γ,p) data smoothly connect by employing the effective missing momentum. Longitudinal-dominant and transverse-dominant data at low and high domains of the missing momentum are now available. Data obtained at various kinematics may contribute to upgrading theoretical ingredients.

ACKNOWLEDGMENTS

We wish to thank the Tohoku University accelerator group and computer group for their assistance in performing the measurements. This work has been partly supported by Grants-in-Aid for Scientific Research (KAKENHI) (Nos. 14540239 and 17540229) from the Japan Society for the Promotion of Science (JSPS).

[1] L. Lapikás, Nucl. Phys. **A553**, 297c (1993).
[2] A. E. L. Dieperink and P. K. A. de Huberts, Ann. Rev. Nucl. Part. Sci. **40**, 239 (1990).
[3] S. Boffi, C. Giusti, and F. D. Pacati, Phys. Rep. **226**, 1 (1993).
[4] M. Hedayati-Poor, J. I. Johansson, and H. S. Sherif, Phys. Rev. C **51**, 2044 (1995).
[5] J. M. Udías, P. Sarriguren, E. Moya de Guerra, E. Garrido, and J. A. Caballero, Phys. Rev. C **51**, 3246 (1995).
[6] J. I. Johansson, H. S. Sherif, and G. M. Lotz, Nucl. Phys. **A605**, 517 (1996).
[7] A. Meucci, C. Giusti, and F. D. Pacati, Phys. Rev. C **64**, 014604 (2001).
[8] J. M. Udías, J. A. Caballero, E. Moya de Guerra, J. R. Vignote, and A. Escuderos, Phys. Rev. C **64**, 024614 (2001).
[9] J. M. Udias, J. A. Caballero, E. Moya de Guerra, J. E. Amaro, and T. W. Donnelly, Phys. Rev. Lett. **83**, 5451 (1999).
[10] J. Gao *et al.*, Phys. Rev. Lett. **84**, 3265 (2000).
[11] A. Meucci, Phys. Rev. C **65**, 044601 (2002).
[12] J. J. Kelly, Phys. Rev. C **56**, 2672 (1997); **60**, 044609 (1999).
[13] M. Radici, A. Meucci, and W. H. Dickhoff, Eur. Phys. J. A **17**, 65 (2003).
[14] J. Ryckebusch, M. Waroquier, K. Heyde, J. Moreau, and D. Ryckbosch, Nucl. Phys. **A476**, 237 (1988).
[15] K. Mori *et al.*, Phys. Rev. C **51**, 2611 (1995).
[16] D. G. Ireland and G. van der Steenhoven, Phys. Rev. C **49**, 2182 (1994).
[17] E. C. Aschenauer, I. Bobeldijk, D. G. Ireland, L. Lapikás, D. Van Neck, B. Schröder, V. Van der Sluys, G. van der Steenhoven, and R. E. Van de Vyver, Phys. Lett. **B389**, 470 (1996).
[18] F. De Smet, H. Ferdinande, R. Van de Vyver, L. Van Hoorebeke, D. Ryckbosch, C. Van den Abeele, J. Dias, and J. Ryckebusch, Phys. Rev. C **47**, 652 (1993).
[19] G. J. Miller *et al.*, Nucl. Phys. **A586**, 125 (1995).
[20] S. V. Springham *et al.*, Nucl. Phys. **A517**, 93 (1990).
[21] C. Giusti and F. D. Pacati, Phys. Rev. C **67**, 044601 (2003).
[22] S. Boffi and M. Radici, Nucl. Phys. **A526**, 602 (1991).
[23] J. E. Amaro, A. M. Lallena, and J. A. Caballero, Phys. Rev. C **60**, 014602 (1999).
[24] J. Ryckebusch, D. Debruyne, W. Van Nespen, and S. Janssen, Phys. Rev. C **60**, 034604 (1999).
[25] J. E. Amaro, M. B. Barbaro, J. A. Caballero, and F. Kazemi Tabatabaei, Phys. Rev. C **68**, 014604 (2003).
[26] M. Hedayati-Poor and H. S. Sherif, Phys. Lett. **B326**, 9 (1994).
[27] J. I. Johansson and H. S. Sherif, Phys. Rev. C **56**, 328 (1997).
[28] A. Meucci, C. Giusti, and F. D. Pacati, Phys. Rev. C **64**, 064615 (2001).
[29] A. Meucci, C. Giusti, and F. D. Pacati, Phys. Rev. C **66**, 034610 (2002).
[30] T. de Forest Jr., Nucl. Phys. **A392**, 232 (1983).
[31] J. A. Caballero, T. W. Donnelly, E. Moya de Guerra, and J. M. Udías, Nucl. Phys. **A632**, 323 (1998).
[32] G. van der Steenhoven, H. P. Blok, E. Jans, M. de Jong, L. Lapikás, E. N. M. Quint, and P. K. A. de Witt Huberts, Nucl. Phys. **A480**, 547 (1988).
[33] M. Leuschner *et al.*, Phys. Rev. C **49**, 955 (1994).
[34] D. J. S. Findlay and R. O. Owens, Nucl. Phys. **A279**, 385 (1977).
[35] A. C. Shotter, S. Springham, D. Branford, J. Yorkston, J. C. McGeorge, B. Schoch, and P. Jennewein, Phys. Rev. C **37**, 1354 (1988).
[36] H. Ruijter, J.-O. Adler, B.-E. Andersson, K. Hansen, L. Isaksson, B. Schroder, J. Ryckebusch, D. Ryckbosch, L. van Hoorebeke, and R. van de Vyver, Phys. Rev. C **54**, 3076 (1996).
[37] T. Tamae, in *Proceedings of the 16th RCNP Osaka International Symposium on Multi-GeV High-Performance Accelerators and Related Technology, Osaka, 1997*, edited by K. Hatanaka, K. Sato, and K. Tamura (World Scientific, Singapore), p. 145.
[38] T. Tamae *et al.*, Nucl. Instrum. Methods A **264**, 173 (1988).
[39] T. Tadokoro, T. Hotta, T. Miura, M. Sugawara, A. Takahashi, T. Tamae, E. Tanaka, H. Miyase, and H. Tsubota, Nucl. Phys. **A575**, 333 (1994).
[40] T. Hotta, T. Tamae, T. Miura, H. Miyase, I. Nakagawa, T. Suda, M. Sugawara, T. Tadokoro, A. Takahashi, E. Tanaka, and H. Tsubota, Nucl. Phys. **A645**, 492 (1999).
[41] J. Friedrich, Nucl. Instrum. Methods **129**, 505 (1975).
[42] M. Sasao and Y. Torizuka, Phys. Rev. C **15**, 217 (1977).
[43] G. C. Li, I. Sick, R. R. Whitney, and M. R. Yearian, Nucl. Phys. **A162**, 583 (1971).
[44] I. Sick and J. S. McCarthy, Nucl. Phys. **A150**, 631 (1970).
[45] J. A. Jansen, R. Th. Peerdeman, and C. de Vries, Nucl. Phys. **A188**, 337 (1972).
[46] B. Dreher, DREPHA 11: a phase-shift calculation code for elastic electron scattering, communicated by J. Friedrich.
[47] J. A. Templon, C. E. Vellidis, R. E. J. Florizone, and A. J. Sarty, Phys. Rev. C **61**, 014607 (1999).
[48] S.-J. Lee *et al.*, Phys. Rev. Lett. **57**, 2916 (1986).
[49] E. D. Cooper, S. Hama, B. C. Clark, and R. L. Mercer, Phys. Rev. C **47**, 297 (1993).
[50] G. Benenti, C. Giusti, and F. D. Pacati, Nucl. Phys. **A574**, 716 (1994).
[51] S. A. Morrow *et al.*, Phys. Rev. C **71**, 014607 (2005).